

CHARACTERIZATION AND ANALYSIS OF GEOMETRIC FEATURES FOR THE WIRE-ARC ADDITIVE PROCESS

Christopher Masuo*, Andrzej Nycz*, Mark W. Noakes*, and Lonnie J. Love*

*Manufacturing Demonstration Facility, Oak Ridge National Laboratory, Knoxville, TN 37932,
USA

Abstract

The wire-arc additive manufacturing (AM) process expands the possibilities of effectively producing large-scale, complex metal objects through high deposition rates at low costs. However, this process is prone to irregularities in geometric features that occur from improper thermal conditions and build parameters that cause uneven build heights. This paper discusses a method to obtain consistent build characteristics and near net shape geometric features for the wire-arc AM process. Process parameters are established for each material printed to ensure characterization of layer build height and even flow in the interior of parts. Various sections of the build including perimeter, infill, and various wall thicknesses require different strategies to correctly build the part. Open-loop build geometry is still not sufficient to build a part to near net shape of the original model. Average layer height is determined and used with adaptive height control to print the correct, modeled height.

Introduction

The wire-arc additive manufacturing (WAAM) process utilizes arc welding (e.g., metal inert gas (MIG), tungsten inert gas (TIG), or plasma arc welding (PAW)) and a gantry or robot system to deposit metal in a layer by layer process [1, 2]. Wire-arc is a direct energy deposition (DED) process with features suitable for medium to large-scale metal printing. Wire-arc is a low cost process both in equipment and material. Welding wire and equipment are inexpensive and easily obtainable. Wire-arc is efficient, environmentally friendly, and a safe process [1-5].

Specifically, a large-scale additive manufacturing (AM) system requires a build envelope where the longest axis has a minimum reach of approximately 1-2m [3]. For a large-scale wire-arc additive system, a robot's high range of motion makes it more suitable for this process and enables the ability to print large parts [6]. Welding robots are also well-known in industry, which requires only slight modifications to an existing industrial automated welding infrastructure. By utilizing a welding robot for a wire-arc additive purpose, metal big area additive manufacturing (mBAAM) is made possible.

Utilizing mBAAM to create large, complex metal objects requires a suitable process for near net shape quality. The challenges are that process parameters need to be determined as well as understanding the characteristics and geometric features that are capable in an arc-wire additive process. Getting started can be difficult; however, this paper provides a guideline to developing, characterizing, and analyzing features that are used as the building blocks for successfully printing near net shape large metal objects. This paper starts with a system description and details how printing was achieved. The method section discusses the features that were studied. Results are

then shown, and adaptive control is addressed to make further improvements. This paper concludes with using these methods to assist in post-process refinement.

System and Printing Process Background

In this paper, an mBAAM system (Figure 1) developed by Wolf Robotics and installed at the Manufacturing Demonstration Facility of Oak Ridge National Laboratory was used. This system uses an ABB 2600 six degree of freedom robot equipped with a Power Wave R500 Lincoln Electric MIG welder. It has an effective build envelope of about 2ft length x 3ft width x 7ft height (0.6m x 1.2m x 2.1m) and a deposition rate ranging from 3.5lbs/hr (1.6kg/hr) to 15lbs/hr (6.8kg/hr). The current system has two torches attached to the end-effector of the robot for multi-material capabilities. Only one torch was used for the experiments done in this paper.

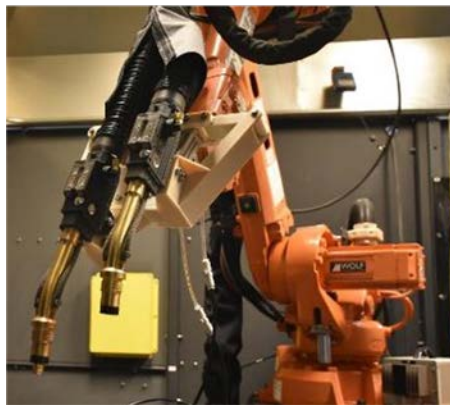


Figure 1. mBAAM Wolf Arc System with multi-torch setup

The process of printing parts using this system has similarities to the common 3D printing methods. A model is created using a CAD software. This model is then saved as an STL to load the object into slicing software. The slicing software used was ORNL Slicer, which was developed by researchers at the Manufacturing Demonstration Facility. The slicer breaks the object into layers of tool paths and generates a g-code file. This g-code is then parsed into a robot path using Wolf Robotics' application add-on for ABB Robot Studios. This printing process is shown in Figure 2.

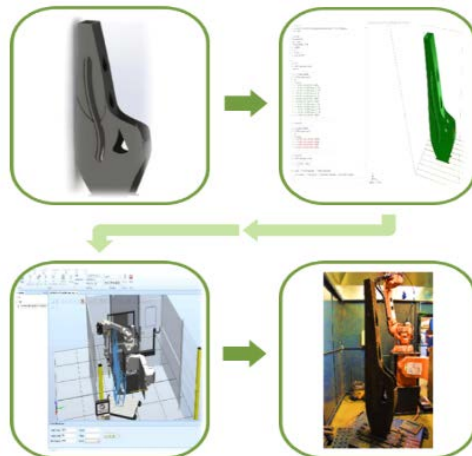


Figure 2. Printing process used for mBAAM system

Methods

A. Straight Walls

Beginning with simple geometry, walls provide the features necessary to understand bead-to-bead forming, surface finish, and geometric dimensions. Before printing a tall wall, welding processes were developed and observed by analyzing the first layer of a single-bead and two-bead thick wall (Figure 3). These welding parameters consist of welding (robot travel) speed, wire-feed speed, and welder specific settings that control the metal transfer. In this case, Lincoln Electric has a waveform library that provides multiple processes. For mild steel printed on the mBAAM system, a short circuit transfer called Surface Tension Transfer (STT) was used for mild steel. STT gives the capability of adjusting heat separately from the wire-feed speed as well as enabling low heat input, reduced of spatter, and better control of the weld bead with increased travel speed [7]. For 410 stainless steel, Power Mode was used for stable arc welding, which is not metal or gas specific. Power Mode also creates a constant output of power [8].

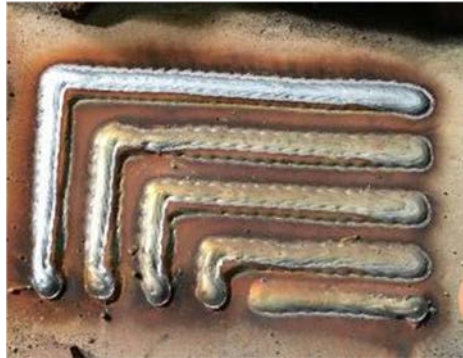


Figure 3. First layer of two-bead thick walls with an L-shape and straight pattern

After analyzing and obtaining welding parameters from the first layer, single-bead and two-bead thick walls were printed. With the single-bead walls, the thickness and height of the bead were measured. These measurements were important for deciding the layer-by-layer dimensions [9]. This data provided a starting bead-to-bead spacing for the two-bead thick walls. When printing a complete two-bead wall, bead-to-bead spacing was adjusted until proper forming between beads was made. Adjustment was achieved by using the ORNL Slicer, which does a center bead-to-bead spacing as shown in Figure 4. Cross-sectional cuts on the walls were done to check for proper forming. Voids appeared when using wide spacing shown in Figure 5. By decreasing the bead-to-bead spacing, these voids were diminished. Once a proper bead-to-bead spacing was obtained, the two bead walls were measured in both height and width. Four-bead thick walls were printed and measured afterwards. The printed one, two, and four-bead thick walls are shown in Figure 6.

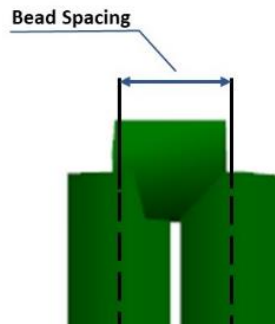


Figure 4. Center bead-to-bead spacing depicted in the ORNL Slicer

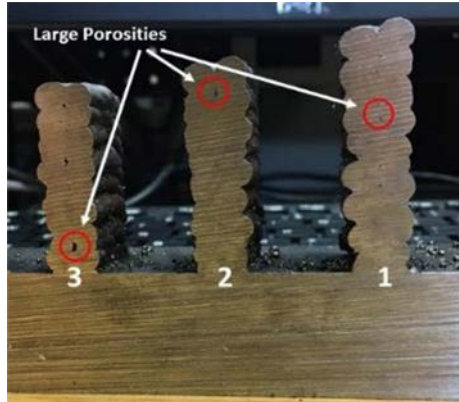


Figure 5. Cross-sectional cuts of a two-bead wall with large voids

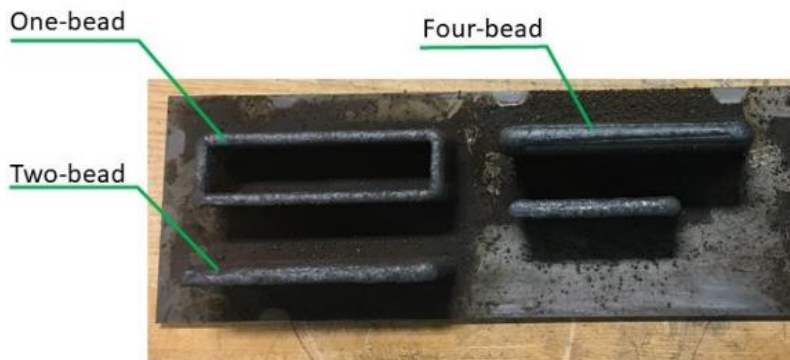


Figure 6. One, two, and four-bead thick walls printed in 410 Stainless Steel

B. Circular Tubes

Another simple shape, circular tubes, may represent internal features such as internal cooling passageways for hot stamping dies or engine block cylinders. This shape was also chosen to understand how the flow of material would change, if any, when encountering a circular path. The objective of printing circular tubes was to observe the size change of the inner and outer diameters. For this part of the experiment, one and two-bead thick circular tubes (Figure 7) were printed. The inner diameter of the tube ranged from 8mm to 30mm with 2mm increments. Measurements on the inner and outer diameters were made to determine an inner and outer offset of the circular tubes. Figure 8 shows the representation of the offsets from the modeled tube. These tubes were also scanned using a FARO Arm Laser Scanner to compare the printed parts with the CAD models.

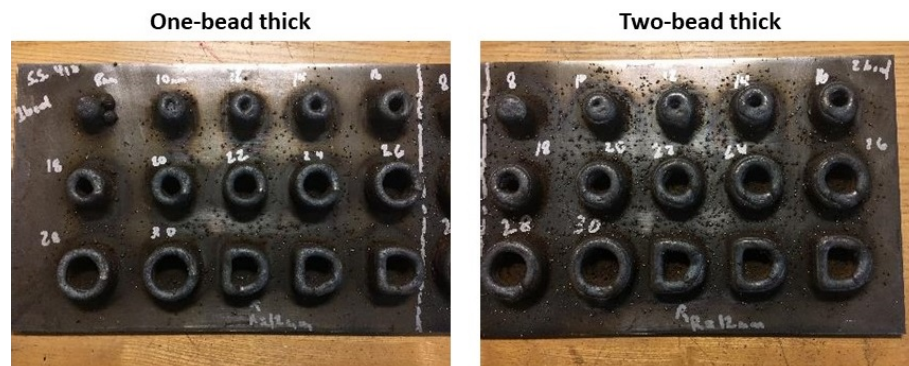


Figure 7. One and two bead thick circular tubes with different inner diameters printed in 410 Stainless Steel

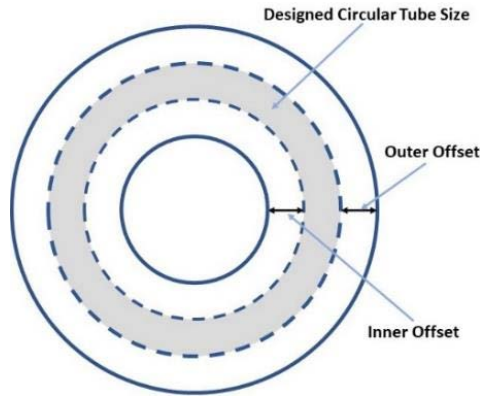


Figure 8. Visualization of the inner and outer offset of a circular tube

C. Square Blocks

Like walls, square blocks have a perimeter and an inset, which are the same as the bead-to-bead spacing shown in Figure 4. In addition to perimeter and insets, infill is introduced when printing a square block. In ORNL Slicer, there are many options for infill patterns (i.e., concentric, line, grid); however, the line pattern was chosen since it decreases the amount of starts and stops when printing as well as provides more heat into the part. When using a line pattern, the linear length infill offset and the sparse infill line distance (Figure 9) were adjusted. The objective was to have flat layers. The right amount of overlapping of beads is necessary to prevent having “hills” and “valleys” in the print.

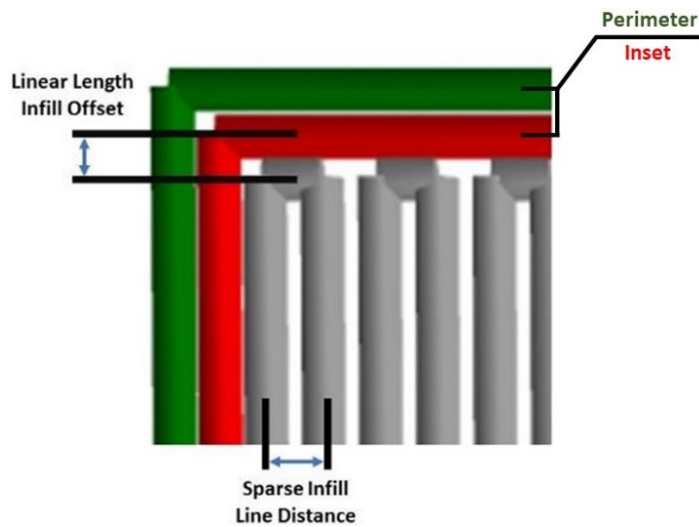


Figure 9. ORNL Slicer representation of the types of bead spacing used in the solid block

Results

Starting with walls, Figure 10 shows a cross-sectional cut of a two-bead thick wall with no voids. The material of this wall was 410 stainless steel, and the bead-to-bead spacing used was 3.2mm. The measurement data obtained from these walls is shown in Table 1. Due to running the first layer with a slower weld speed to heat up the build plate, the first layer’s height and width (thickness) was measured in addition to measuring the wall when it was completed. In Table 1, a height per layer of the walls was determined to input back into the slicer, which ensures that a part

will print to the correct height. This value will also be used with adaptive, closed-loop control to minimize the error in height when printing.



Figure 10. 410 stainless steel, two-bead thick wall without any voids

Table 1. Average measurement data from a one, two, and four- bead thick stainless-steel wall

Base Layer: Height and Width								
	One Bead Wall			Two Bead Wall			Four Bead Wall	
Average:	3.39	9.22		5.12	11.48		7.70	17.71
Deviation	-3.61			-1.88			0.70	
Offset+-		3.009			2.54			2.455
End of Layer 20: Height and Width								
	One Bead Wall			Two Bead Wall			Four Bead Wall	
Average:	41.75	8.23		56.29	11.34		70.10	18.06
Total Height Deviation	-26.05			-11.51			2.30	
Height per Layer	2.02			2.69			3.28	
Layer Height Deviation	-1.18			-0.51			0.08	
Offset+-		2.515			2.469			2.63

Figure 11 shows a graph of the printed inner and outer diameters and offsets of the circular tube compared to the CAD model, and Figure 12 shows the scanned tubes and CAD model comparison. In Figure 11a, the comparison between the actual and designed tubes have a linear relationship for both the inner and outer diameters. There was not a drastic difference in the inner and outer diameters between the one and two-bead thick tubes. In Figure 11b, the inner offset was larger than the outer offset by approximately 1.5mm. This indicates that the inner diameter shrinks more than the outer diameter. When designing features such as cooling channels, the CAD model's bore features should be larger to avoid the cooling channels from closing mid print.

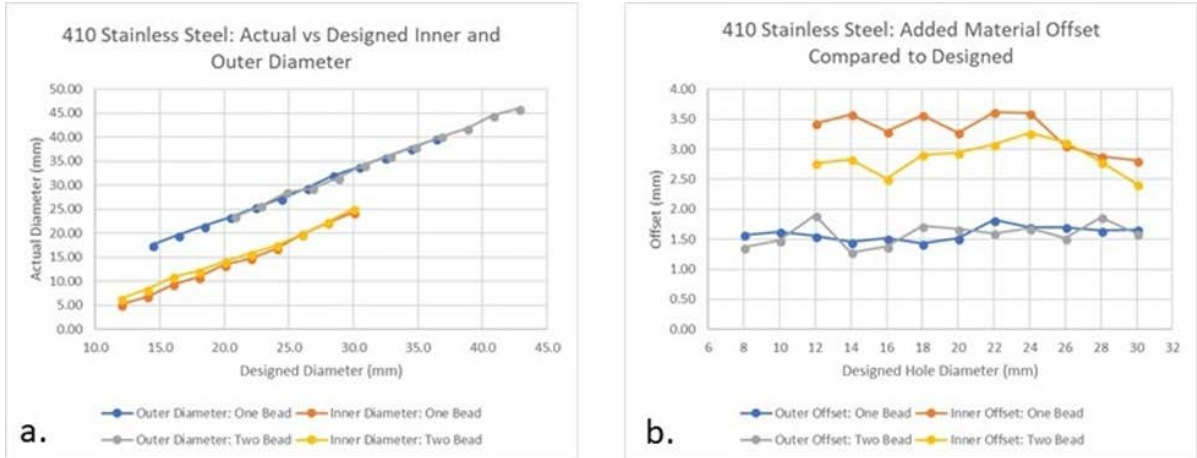


Figure 11. Comparison of the as designed tubes to the actual tubes in 410 stainless steel. a.) Inner and outer diameter plot. b.) inner and outer offsets vs. the inner diameter of the tubes

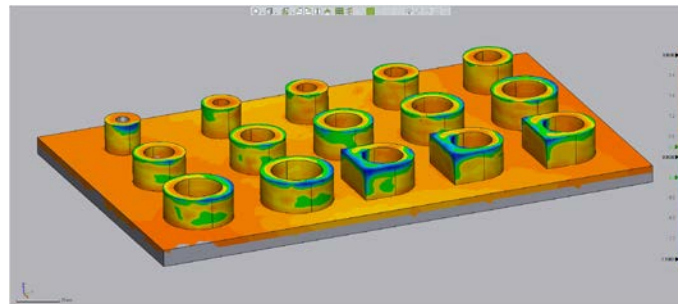


Figure 12. Scan of the tubes compared with the CAD model. This was done with Geomagic Control X.

The results for the square block was more observational. Initial blocks had distinct overbuilding (Figure 12a) in the first few layers. In Figure 12b, a nice, flat square block was printed with 15 layers out of 410 stainless steel. The perimeter and inset value used was 3.2mm, which is the same as the bead-to-bead spacing obtained from the straight walls. The sparse infill line distance used was 4mm with a linear infill length offset of 2.4mm. Due to having one perimeter and one inset, the layer height used was 2.69mm, which was obtained from Table 1. These were successfully printed without adaptive control; however, if the block was significantly taller, the error in the height would accumulate, leading to sloped layers.

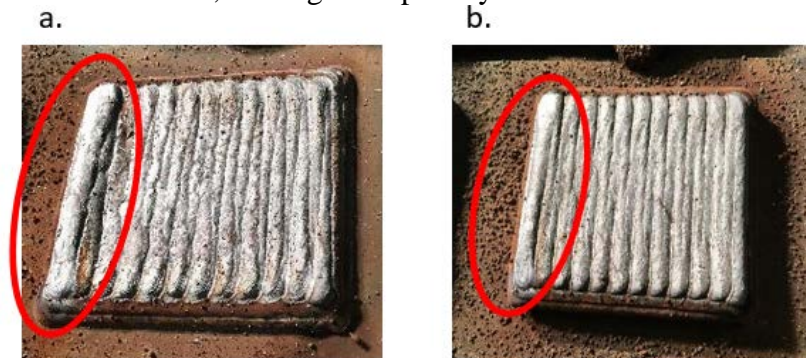


Figure 13. a.) Block with too large overbuild in just two layers, b.) No overbuild with 15 layers in.

These parts were relatively short (40mm tall) and did not experience an uneven build. When printing a part larger than 100mm, overbuilding accumulates leading to uneven surfaces and the possibility for the part failing completely. For large-scale printing, it is crucial to have

consistent layer heights with flat surfaces to achieve a near net shape geometry. An open-loop control system is not able to do this, which makes a closed-loop system necessary [10].

Wire-arc additive systems that use a closed-loop control system tend to use vision-based sensors and process this information to adapt for the next layer. In the mBAAM Wolf Arc system, closed-loop control is achieved by using wire tracking. Wire tracking measures the impedance of the welding arc and corrects the wire stick-out (Figure 14) based on a specified current [11]. By having the end of the stick-out to be the tool center point (TCP) of the robot, the height of the build can be determined during metal deposition. By combining both feedback and feedforward control, adaptive height control can be achieved using minimal hardware. This also results in having height correction during deposition, creating flat, smooth layers. The adaptive height control process is shown in Figure 15. Basically, the welding speed of the robot either slows down or speeds up depending on whether there is an overbuilt or underbuilt surface. Wire-feed speed is held constant, allowing metal to deposit more or less depending on the surface height. Drastic improvements can be seen in tall walls shown in Figure 16.

By combining the geometries used in this paper, the process of printing a complex shape was simplified. Figure 17 shows the integration of all these geometries. This part was a sample hot stamping tool with integrated cooling channels printed using 410 stainless steel. Using adaptive control also resulted in a smooth, flat surface. The final result led to a more near net shape geometry.

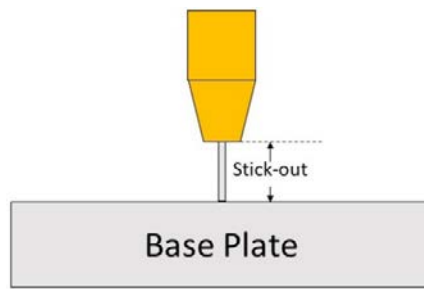


Figure 14. MIG wire stick-out, which is the distance between the end of the contact tip and the base plate

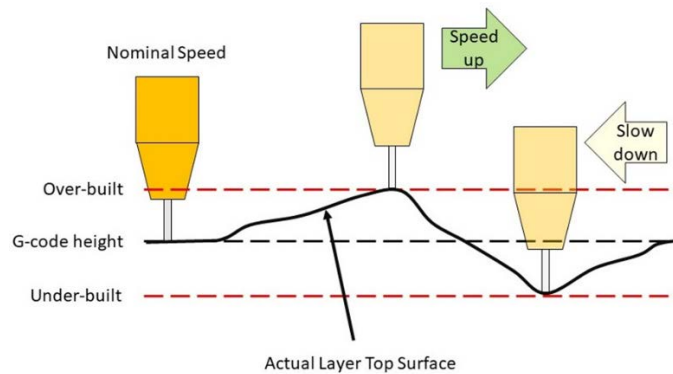


Figure 15. Drawing of the adaptive control process

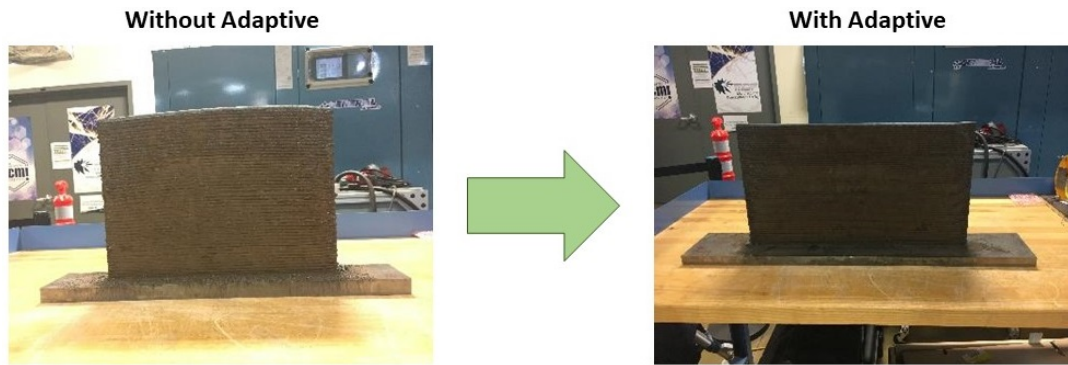


Figure 16. Comparison between a non-adaptive printed wall and an adaptive printed wall

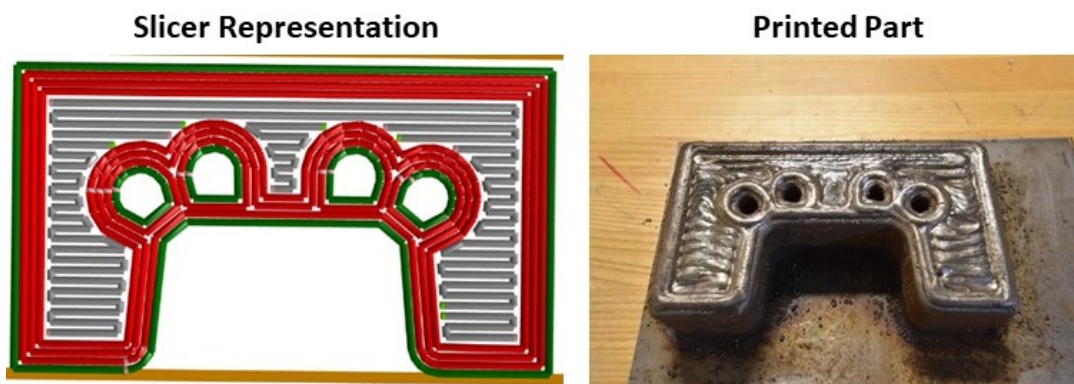


Figure 17. Hot stamping tool with sliced image on the left and printed part on the right

Conclusion

With simple geometries, characterization of wire-arc features was broken down into a simple process. By understanding these geometries, complex shapes with near net shape geometries can be developed and achieved with ease. The obtained data also assists with post-process machining, which is used to refine the printed part to produce the actual designed part with minimal material waste.

Acknowledgements

This material is based upon work supported by the U.S. Department of Energy, Office of Science, Office of Energy Efficiency & Renewable Energy, Advanced Manufacturing Office, under contract number DE-AC05-00OR22725.

References

1. Williams, S. W., Martina, F., Addison, A. C., Ding, J., Pardal, G., & Colegrove, P. (2016). Wire Arc Additive Manufacturing. *Materials Science and Technology*, 32(7), 641-647. doi:10.1179/1743284715y.0000000073
2. Lockett, H., Ding, J., Williams, S., & Martina, F. (2017). Design for Wire Arc Additive Manufacture: Design rules and build orientation selection. *Journal of Engineering Design*, 28(7-9), 568-598. doi:10.1080/09544828.2017.1365826
3. Nycz, A., Adediran, A. I., Noakes, M. W., & Love, L. J. (2016). Large-Scale Metal Additive Techniques Review. In *Solid Freeform Fabrication 2016: Proceedings of the 27th Annual International Solid Freeform Fabrication Symposium - An Additive Manufacturing Conference*. Retrieved from <http://sffsymposium.engr.utexas.edu/sites/default/files/2016/161-Nycz.pdf>
4. Li, F., Chen, S., Wu, Z., & Yan, Z. (2018). Adaptive process control of wire and arc additive manufacturing for fabricating complex-shaped components. *The International Journal of Advanced Manufacturing Technology*. doi:10.1007/s00170-018-1590-0
5. Ding, D., Pan, Z., Cuiuri, D., & Li, H. (2015). A multi-bead overlapping model for robotic wire and arc additive manufacturing (WAAM). *Robotics and Computer-Integrated Manufacturing*, 31, 101-110. doi:10.1016/j.rcim.2014.08.008
6. Mehnen, J., Ding, J., Lockett, H., & Kazanas, P. (2010). Design for Wire and Arc Additive Layer Manufacture. *Proceedings of the 20th CIRP Design Conference, Nantes France, 19-21 April, 2010*. Ed. A. Bernard.
7. Lincoln Electric. (n.d.). *Surface Tension Transfer (STT)* [Brochure]. Author. Retrieved from <https://www.lincolnelectric.com/assets/US/EN/literature/NX220.pdf>
8. Lincoln Electric. (n.d.). *Power Mode* [Brochure]. Author. Retrieved from <https://www.lincolnelectric.com/assets/US/EN/literature/NX260.pdf>
9. Xiong, J., Yin, Z., & Zhang, W. (2016). Closed-loop control of variable layer width for thin-walled parts in wire and arc additive manufacturing. *Journal of Materials Processing Technology*, 233, 100-106. doi:10.1016/j.jmatprotec.2016.02.021
10. Geng, H., Xiong, J., Huang, D., Lin, X., & Li, J. (2015). A prediction model of layer geometrical size in wire and arc additive manufacture using response surface methodology. *The International Journal of Advanced Manufacturing Technology*, 93(1-4), 175-186. doi:10.1007/s00170-015-8147-2
11. Nycz, A., Noakes, M. W., Richardson, B., Messing, A., Post, B., Paul, J., . . . Love, L. J. (2017). Challenges in Making Complex Metal Large-scale Parts for Additive Manufacturing: A Case Study Based on the Additive Manufacturing Excavator. In *Solid Freeform Fabrication 2017: Proceedings of the 28th Annual International Solid Freeform Fabrication Symposium – An Additive Manufacturing Conference*. Retrieved from <http://sffsymposium.engr.utexas.edu/sites/default/files/2017/Manuscripts/ChallengesinMakingComplexMetalLargeScalePar.pdf>